ELSEVIER

Cell Calcium 41 (2007) 77–86

cell calcium

www.elsevier.com/locate/ceca

Purinergic signalling and intercellular Ca^{2+} wave propagation in the organ of Corti

Valeria Piazza [a,1], Catalin D. Ciubotaru [a,1], Jonathan E. Gale [b], Fabio Mammano [a,c,*]

[a] *Venetian Institute of Molecular Medicine, Foundation for Advanced Biomedical Research, via G. Orus 2, 35129 Padova, Italy*
[b] *Department of Physiology and Centre for Auditory Research, UCL Ear Institute, 332 Gray's Inn Road, London WC1X 8EE, UK*
[c] *Department of Physics "G. Galilei.", University of Padova, via Marzolo 8, 35131 Padova, Italy*

Received 1 March 2006; received in revised form 9 May 2006; accepted 14 May 2006
Available online 7 July 2006

Abstract

Extracellular ATP is a key neuromodulator of visual and auditory sensory epithelia. In the rat cochlea, pharmacological dissection indicates that ATP, acting through a highly sensitive purinergic/IP_3-mediated signaling pathway with (little or) no involvement of ryanodine receptors, is the principal paracrine mediator implicated in the propagation of calcium waves through supporting and epithelial cells. Measurement of sensitivity to UTP and other purinergic agonists implicate $P2Y_2$ and $P2Y_4$ as the main P2Y receptor isoforms involved in these responses. Ca^{2+} waves, elicited under highly reproducible conditions by carefully controlling dose (1 μM) and timing of focal agonist application (0.2 s), extended over radial distance greater than 160 μm from the source, identical to those activated by damaging single outer hair cells. Altogether, these results indicate that intercellular calcium waves are a robust phenomenon that confers a significant ability for cell–cell communication in the mammalian cochlea. Further ongoing research will reveal the roles that such Ca^{2+} waves play in the inner ear.

Keywords: Cochlea; Hearing; Calcium waves; Calcium oscillations; IP_3; P2 receptors; Intercellular communication

1. Introduction

Extracellular signalling by purine nucleotides has long been associated with sensory systems, where ATP acts as a co-transmitter and/or neuromodulator [1]. Purinergic receptors of the G protein-coupled (P2YR) type, as well as of the ionotropic type (P2XR) [2] are widely distributed on inner ear structures [3,4].

Currently, seven subtypes of the P2X family ($P2X_{1–7}$) and eight subtypes of the P2Y family ($P2Y_{1–2}$, $P2Y_4$, $P2Y_6$ and $P2Y_{11–14}$) have been cloned and functionally characterised, albeit typically in expression systems rather than native tissue [5]. As non-selective cation channels, P2XRs provide direct routes for Ca^{2+} entry into the cell cytoplasm, whereas P2YRs either activate phosholipase C (PLC) and release intracellular Ca^{2+} or affect adenylyl cyclase and alter cAMP levels [6].

In the mammalian cochlea, the organ of Corti comprises a polarized epithelium that contains sensory receptors, the hair cells, in which ATP has been shown to affect Ca^{2+} homeostasis [7]. Sensory hair cells are surrounded by various types of supporting cells, including Deiters' [8–10], Hensen's [11] and pillar cells [12], which all respond to focal application of ATP with a transient elevation of the intracellular free Ca^{2+} concentration ($[Ca^{2+}]_i$). Cochlear supporting cells and adjacent epithelial (Böttcher's and Claudius') cells are considered essential constituents of an epithelial network that participates in the regulation of the unique ionic composition of cochlear extracellular fluids [13]. Hensen's and Deiters' cells, the two main types of supporting cells in the organ of Corti [14,15], are highly permeable to K^+ [16,17] which is found at unusually high concentration in endolymph, the fluid bathing the apical surface of the organ of Corti [18]. K^+ ions flow into the organ of Corti as they are the major component

* Corresponding author. Tel.: +39 049 7923 231; fax: +39 049 7923 266.
E-mail address: fabio.mammano@unipd.it (F. Mammano).
[1] The authors contributed equally.

0143-4160/$ – see front matter © 2006 Elsevier Ltd. All rights reserved.
doi:10.1016/j.ceca.2006.05.005

of the hair cell mechanoelectrical transduction current [19-22]. Purinergic signalling in the cochlea can affect several essential functions, from ion homeostasis to active mechanical amplification by the outer hair cells [23,24]. Notably, the level of ATP in cochlear fluids increases in response to modest sound over-stimulation [25]. ATP release from marginal cells in the stria vascularis has been proposed to exert a homeostatic regulatory mechanism [26], promoting K^+ efflux from scala media and a G protein-mediated reduction of K^+ import into the endolymph from stria vascularis [27]. An expected outcome of both of these effects is a reduction in cochlear sensitivity in noisy environments.

Mechanical stimulation of many cell types induces transient rises in $[Ca^{2+}]_i$ that can spread from cell to cell in a wave-like pattern by the release of an extracellular nucleotide intermediate [28]. Indeed, nucleotides are frequently released into the extracellular space as a consequence of cell damage and, once in the pericellular milieu, they can activate P2 nucleotide receptors or be rapidly hydrolyzed by ecto-ATPases and ectonucleotidases [29]. Using neonatal organotypic cultures from rat inner ear [30–32], we have recently shown, in response to sensory hair cell damage, activation of Ca^{2+} oscillations and ATP-dependent propagation of Ca^{2+} waves through cochlear supporting and epithelial cells that surround the damaged hair cells. ATP concentrations above about 15 nM, similar to that measured in noise damaged cochlea, reliably elicit Ca^{2+} oscillations in the same organ preparation [33].

Extracellular ATP possesses all the properties of a bona fide fast-acting intercellular messenger: (a) it is released in a controlled fashion, (b) ligates specific plasma membrane receptors coupled to signal transduction and (c) is quickly degraded to terminate its actions [29]. However, an alternative concept has been proposed for the mechanism of the Ca^{2+} wave propagation between glial [34] and epithelial cells [35] that, like cochlear supporting cells [36–38], are highly coupled by gap junctions. In this paradigm, Ca^{2+} waves are sustained by the intercellular diffusion of second messengers through gap junctions, with subsequent release of Ca^{2+} from intracellular stores [39]. As Ca^{2+} may permeate gap junctions [40] but is heavily buffered in the cytosol [41], IP_3 has been proposed as a better intercellular messenger in epithelial cells [35,42], hepatocytes [43] and glial cells [44–48]. In the retina, both mechanism seem active: Ca^{2+} wave propagation among astrocytes depends on gap junctional communication while propagation between astrocytes and Müller cells involves purinergic signalling [49].

The contribution of gap junction communication to the propagation of cochlear Ca^{2+} waves is not explored in this paper and will be dealt with in a separate publication. In this work, we have analyzed the responses to different types of stimuli capable of eliciting Ca^{2+} waves in the organ of Corti. Experiments were performed in low divalent cation solutions, thus direct contribution from Ca^{2+} entry through ionotropic P2X receptors can be excluded. Our results implicate $P2Y_2$ and $P2Y_4$ receptors acting via the PLC-IP_3 signal transduction pathway with little or no contribution from ryanodine-sensitive Ca^{2+} stores.

2. Methods

2.1. Organ cultures

Cochleas were dissected from postnatal days 1–2 Sprague–Dawley rat pups in ice-cold Hepes-buffered (10 mM, pH 7.2) Hanks' balanced salt solutions (HBSS, Sigma, Milan, Italy) and placed onto glass coverslips coated with 10 μg ml^{-1} of CellTak (Becton Dickinson, Milan, Italy), as described [33]. Cultures were incubated in Dulbecco's modified Eagle's medium DMEM/F12 (Invitrogen, Leek, The Netherlands), supplemented with FBS 5% and maintained at 37 °C for 1 day. During experiments, cultures were continuously superfused at 2 ml min^{-1} with standard extracellular solution (ECS) containing 138 mM NaCl, 5 mM KCl, 2 mM $CaCl_2$, 0.3 mM NaH_2PO_4, 0.4 mM KH_2PO_4, 10 mM Hepes-NaOH and 6 mM D-glucose (at pH 7.25; 320 mOsm). Before recording, cultures were switched to DFM (as above, but with 0 μM Ca^{2+}, 0 μM Mg^{2+} and 100 μM EGTA) or LCS (as above, with 0 Ca^{2+}, 0 Mg^{2+} but no added EGTA to prevent run-down effects in experiments that required ATP applications lasting longer than 2 min) and were returned to ECS in the interval between successive records.

All experiments were performed at room temperature (22–24 °C).

2.2. Drug delivery

Thapsigargin and ryanodine (Calbiochem, Darmstadt, Germany) were dissolved at the indicated concentrations respectively in LCS and ECS and applied through the perfusion. Focal pressure-applications of purine/pyrimidine derivatives were performed using glass micro-capillaries (puff pipettes) that were pulled to a tip of approximately 1 μm on a vertical puller, similarly to patch clamp electrodes (PP80, Narishige, Tokyo, Japan). Pipettes were filled with the compound of interest, dissolved in DFM or LCS, and placed near the target cell. A 6 psi pressure was applied at the back of the pipette by delivering a transistor–transistor logic (TTL) pulse of carefully controlled duration to a Pneumatic PicoPump (PV800, World Precision Instruments, Sarasota, FL, USA) under software control. All cells tested responded to ATP, whereas no response was detected when ATP (or other agonists) was omitted from the puff pipette solution, indicating that mechanical activation of the cells was negligible.

2.3. Mechanical stimulation

Controlled mechanical stimuli were delivered by manually micro-manipulating a glass micropette into close proximity (~1 μm) to a selected outer hair cell, thereafter oscillating the pipette tip for 0.2 s at 100 Hz with an amplitude of 5 μm.

Pipette movement was generated by a piezo-electric actuator (PV820, Physik Instrumente, Karlsruhe, Germany) under software control.

2.4. Calcium imaging

Cochlear organotypic cultures were incubated with the membrane-permeable AM-ester derivative of fura-2 (10 μM) for 30 min at room temperature in the presence of Pluronic F-127 (0.01%, w/v) and sulphinpyrazone (250 μM), and washed in ECS for 20 min before imaging. Fura-2 fluorescence was excited alternatively at 360 nm (isosbestic point) and 380 nm by a fast-switching monochromator (Polychrome IV, TILL Photonics, Martinsried, Germany). Fluorescence emission was selected at around 510 nm using an interference filter (Chroma D510/40m, Rockingham, VT) to form fluorescence images on a scientific-grade CCD camera (SensiCam; PCO Computer Optics GmbH, Kelheim, Germany) using Olympus Lum Plan FL 20×, 40× and 60× water-immersion objectives (NA 0.95, 0.8 and 0.9, respectively) on a BX51WI upright microscope (Olympus, Tokyo, Japan). The image acquisition software was developed in the laboratory and is described in Ref. [50]. Fura-2 data are shown either as background-subtracted 360/380 nm ratios (R) or as ratio changes ($\Delta R = R - R_0$), where R_0 is the pre-stimulus ratio and R is the ratio at time t.

2.5. Analysis

Data were analysed off-line using customised routines developed under the Matlab 7.1 programming environment (The MathWorks, Natick, MA). To measure the spread of Ca^{2+} transients evoked by focal stimuli, either mechanical (Fig. 1) or chemical (Fig. 2), consecutive images in the fura-2 ratiometric sequence were subtracted, effectively creating a differential image set. The newly responding cells were highlighted by selecting all pixels with values above a given acceptance threshold in the difference image. This procedure yielded clearly discernible ring-like patterns of advancing wave fronts, as shown in Fig. 1B. Classically, propagating Ca^{2+} transients are represented by computing average fluorescence signals within regions of interests (ROIs, Fig. 1A) placed on individual cells along a line departing from the point source. This results in a collection of time plots in which Ca^{2+} elevation delay increases with distance from the source (Fig. 1C). To avoid the tedious placement of individual ROIs, we designed a computer algorithm that automatically computed distances d_{ij} (arrowed in B) from the source point to points on the wave front in each difference image (subscripts ij designate pixel coordinates). Probability histograms were then derived by counting the number of wave front pixels found at a given distance d_{ij}. This is demonstrated by the histograms in Fig. 1D, which were derived from the corresponding difference frames in Fig. 1B. For each difference frame, the abscissa, d_{max}, of the histogram peak was selected and R was averaged over all pixels found at this distance from the source. Fig. 1E shows wave amplitude, A_{max}, i.e. the average value R at d_{max}, as a function of d_{max}. Fig. 1F shows d_{max} as a function of time. Wave speed was estimated from the slope of linear least square fits to these data point distributions.

Results are given as mean ± standard error of the mean (S.E.M.), unless otherwise stated.

3. Results

3.1. Propagation of intercellular Ca^{2+} waves in the outer sulcus of the organ of Corti

To study Ca^{2+} wave propagation in the organ of Corti, perfusion was switched to DFM, a commonly used medium (e.g., see Ref. [51]) virtually devoid of divalent ions (see Section 2.1) 2 min prior to stimulation, and then stopped altogether. Cochlear cultures were kept in DFM for the duration of the recording (generally less than 1 min) and were subsequently returned to ECS, a Ca^{2+}-containing Mg^{2+}-free medium, in the interval between repeated stimulations. To exclude run-down effects, we elicited two consecutive waves in DFM, which served as control for statistical analysis.

In DFM, pressing a micropipette against a selected outer hair cell for ∼0.2 s under software control resulted in Ca^{2+} waves that propagated to distances in excess of 160 μm through the outer sulcus region, a syncytium formed primarily by supporting (Hensen's) and epithelial (Böttcher's and Claudius') cells [14] (Fig. 1A–D). In this range, wave amplitude, A_{max}, and wave speed, s, were constant (Fig. 1E and F). Typical values were $A_{max} \approx 1.5$ (in fura-2 ratio units) and $s \approx 15\ \mu m\ s^{-1}$. Similar waves were elicited by 0.2 s focal application of 1 μM ATP from a puff pipette (Fig. 2A–C), confirming the implication of ATP in calcium wave propagation through cochlear supporting cells [33]. Ca^{2+} signals were never detected when ATP was omitted from the solution filling the puff pipette ($n = 7$). Pooled results indicate that A_{max} and s were not significantly different for the two wave initiation modalities (Fig. 2D).

3.2. IP_3-sensitive intracellular calcium stores are required for ATP-dependent Ca^{2+} responses

In a variety of cells, including cochlear outer sulcus cells [33], stimulation by hormones and neurotransmitters evokes oscillations in cytosolic Ca^{2+}, often accompanied by spreading of intercellular Ca^{2+} waves [52], which propagate through the cytosol of individual cells using either ryanodine or IP_3 receptors [53]. To test the dependence of Ca^{2+} signals evoked by ATP on endoplasmic reticulum (ER) stores, cochlear organotypic cultures bathed in LCS (see Section 2.1) were exposed to thapsigargin, a blocker of the Ca^{2+}-ATPase (SERCA) pump. ATP (100 nM) was applied briefly from a puff pipette, as a control, followed by co-application of ATP (100 nM) and thapsigargin (200 nM) through the

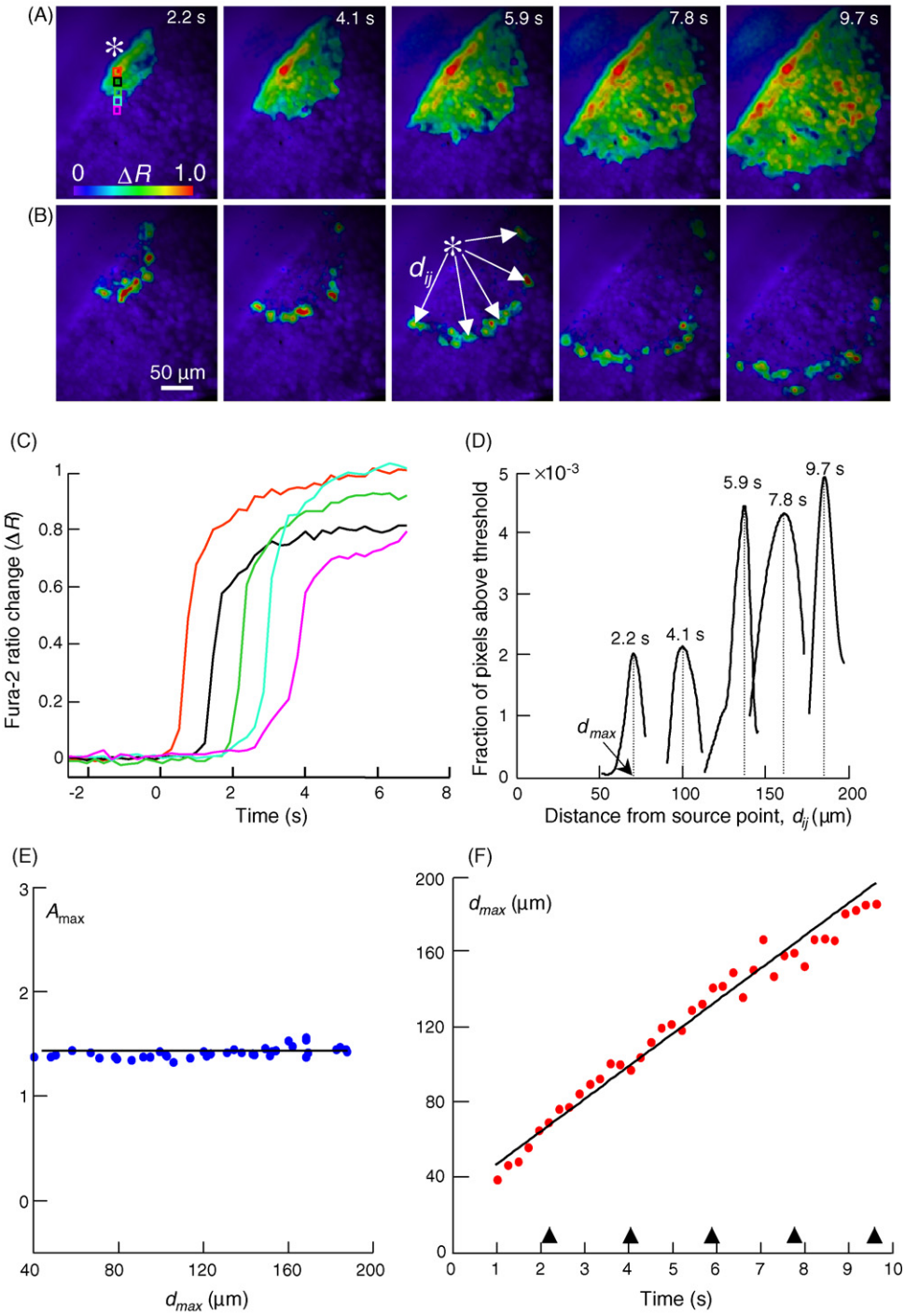

Fig. 1. Intercellular Ca^{2+} signaling in cochlear supporting cells. (A) Five pseudocolor images from one representative experimental record, showing propagating Ca^{2+} transients induced by mechanical stimulation of a single outer hair cell (asterisk). Regions of interest (ROIs) are shown superimposed over five selected supporting cells in the first image (the time of image capture, measured from stimulus onset is shown in the top right corner of each panel). (B) Subtraction images corresponding to the sequence in (A). By subtracting two subsequently recorded images, the newly responding cells are highlighted. Arrows on the third subtraction image indicate wavefront displacements, i.e. distances d_{ij} of wavefront pixel ij from the point of stimulation (asterisk). (C) Fura-2 ratio changes, R, from the ROIs in (A); trace and ROI colours are matched. (D) Graphical representation of the fractions of pixels above a fixed ratio threshold calculated for the five frames in (B); the abscissa of each pixel distribution peak represents the distance, d_{max}, at which the probability of finding ratio differences above threshold is maximal; distances are measured from the point of origin of the wave (asterisk in B). (E) Amplitude (A_{max}) of fura-2 ratio signal vs. d_{max}; there is no significant decrease of the wavefront $[Ca^{2+}]_i$ with distance from the source. (F) Plot of d_{max} vs. time; the slope of the linear best fit to the data was used to estimate wave speed, s, from each record. Arrowheads indicate the timing of capture for the frames shown in (A).

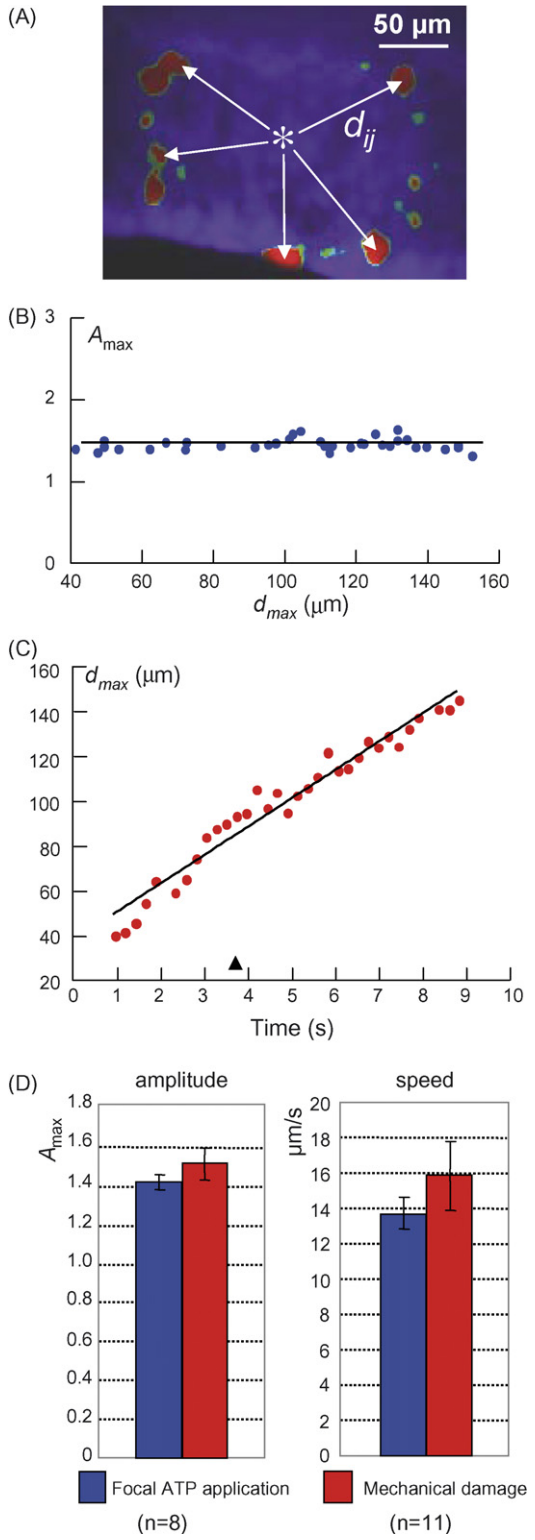

Fig. 2. Calcium waves evoked by focal ATP application. (A) Subtraction image captured ~3.8 s after 0.2 s focal pressure application of 1 μM ATP from a puff pipette placed ~5 μm above the tissue (asterisk). Amplitude (B) and speed (C) of the ATP-evoked waves are compared to those of mechanically evoked waves in (D). Error bars are standard deviation (S.D.). Arrowhead in (C) indicates the timing of capture for the frame shown in (A).

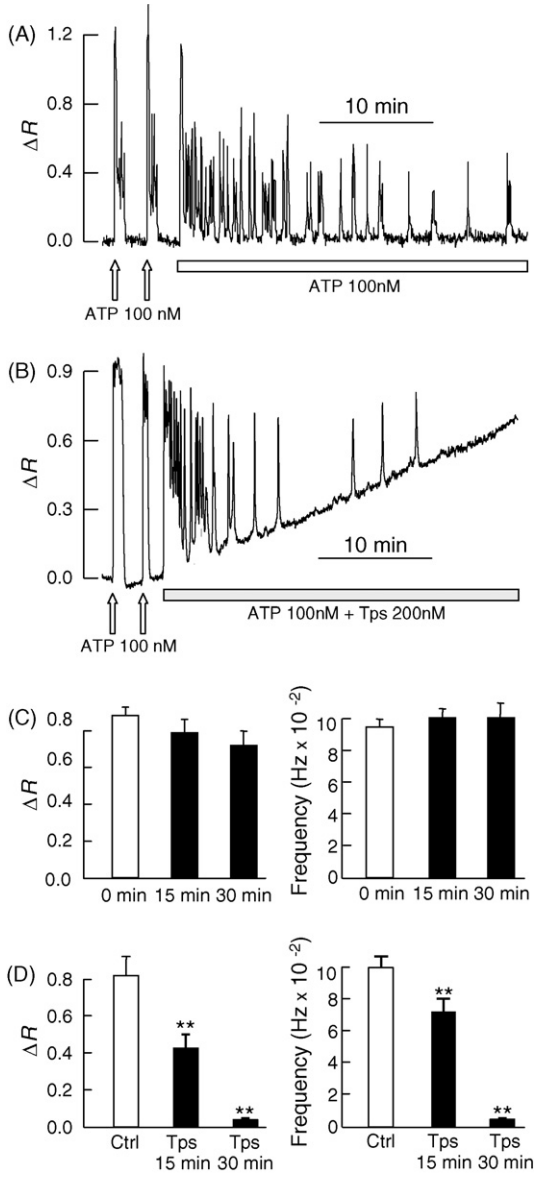

Fig. 3. Thapsigargin suppresses calcium oscillations evoked by ATP. (A and B) Responses evoked by two consecutive brief applications of 100 nM ATP (upward arrows) followed by prolonged ATP application (A, empty bar) or co-application of 100 nM ATP and 200 nM thapsigargin (B, gray bar). Thapsigargin slowly and irreversibly reduced oscillation amplitude and frequency. (C) Pooled data showing quantification of the changes in peak-to-peak fura-2 ratio (ΔR) amplitude (left) and frequency (right) evoked by repeated application of 100 nM ATP (1 min) at 15 min intervals ($n = 30$ cells). (D) Same as (C), before (Ctrl, empty bars, $n = 9$ cells) and during thapsigargin application (Tps, black bars, $n = 6$). **Significant differences at $p < 0.01$.

superfusate. In the presence of thapsigargin, the amplitude and frequency of Ca^{2+} oscillations evoked by ATP, and measured from regions of interest (ROIs) placed within individual cells, declined far more rapidly than in controls until, after about 20 min, only sporadic oscillations were left (Fig. 3). However, oscillations were largely unaffected when cultures were incubated in 50 μM ryanodine for at least 10 min (Fig. 4). Consistently, stimulation with caffeine (10 mM) failed to evoke measurable fura-2 signals ($n = 5$, data not

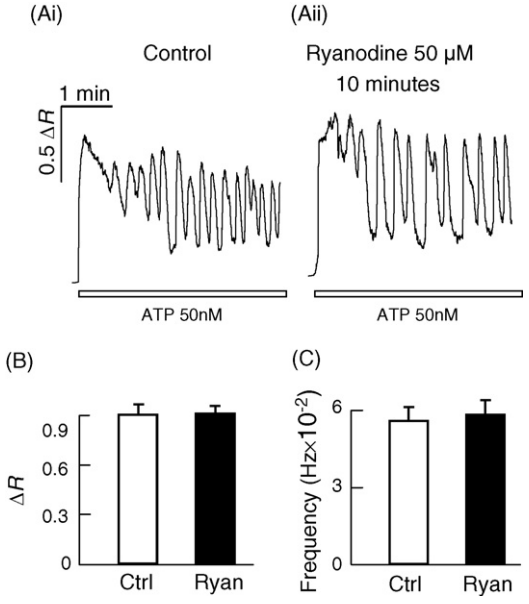

Fig. 4. ATP-evoked calcium responses are not affected by ryanodine. Fura-2 ratio changes evoked by 50 nM ATP (empty bars) before (Ai) and 10 min after incubation with 50 μM ryanodine (Aii). Pooled data from $n = 15$ cells in three different cultures, showing that ryanodine did not affect amplitude (B) or frequency (C) of Ca^{2+} oscillations.

shown). Also, in the same preparation, we have shown that the phospholipase C inhibitor U73122 significantly reduced both the maximal Ca^{2+} response and the frequency of the ATP-induced $[Ca^{2+}]_i$ oscillations [33]. Thus we confirm here that ATP-induced calcium oscillations in cochlear support cells are mediated by PLC-dependent activation of inositol triphosphate (IP_3) sensitive Ca^{2+} channels in the ER.

3.2.1. *Pharmacological profiling of P2Y receptors*

The $[Ca^{2+}]_i$ responses described so far in this work were obtained in low divalent cation solutions using ATP concentrations up to 1 μM, and therefore could be ascribed primarily to P2YRs rather than Ca^{2+} influx via P2X receptor channels [54]. Some P2YRs are activated principally by nucleotide diphosphates ($P2Y_{1,6,12–13}$), while others are activated mainly by nucleotide triphosphates ($P2Y_{2,4}$). Some P2YRs are activated by both purine and pyrimidine nucleotides ($P2Y_{2,4,6}$), and others by purine nucleotides alone ($P2Y_{1,11–13}$). With respect to the signal transduction pathway, each P2YR binds to a single heterotrimeric G protein (typically $G_{q/11}$), although $P2Y_{11}$ can couple to both $G_{q/11}$ and G_s, whereas $P2Y_{12}$ couples to G_i [6]. $P2Y_1$ and $P2Y_2$ are coupled to stimulation of phospholipase C-β and inhibition of adenylate cyclase via G_q/11 and G_i proteins, respectively [2]. $P2Y_4$ and $P2Y_6$ seem to only couple to phosphoinositide breakdown, whereas $P2Y_{11}$ rather surprisingly stimulates activation of both the phosphoinositide and the adenylate cyclase pathways [29].

P2 receptor pharmacology is complex. All of the P2YRs are activated by ATP, but at $P2Y_6$ receptors, UTP is a more potent agonist [55–58], whereas ATP and UTP are equipotent at *rat* $P2Y_2$ and $P2Y_4$ receptors [59,60]. At $P2Y_1$, UTP is inactive and ADP is reported to be equipotent or even more potent than ATP [61,62]; at $P2Y_{11}$ ATP is more potent than ADP and UTP is inactive [63]. Four major isoforms of P2YRs ($P2Y_{1,2,4,6}$) were detected in a mRNA RT-PCR assay from rat whole cochlea samples [33]. Here, to refine the expression profile of the P2YRs, we performed a number of experiments with agonists that have been reported to activate the various receptor isoforms with different potency. Fura-2 fluorescence ratio changes evoked by ATP were compared to responses evoked by stimulation with 2-MeSATP (selective for $P2Y_1$), ATPγS and UDP (acting preferentially on $P2Y_6$) [2,64].

When ATP was applied focally from a puff pipette for periods greater than 20 s at concentrations as low as 20 nM, repetitive increases of $[Ca^{2+}]_i$ were observed (Fig. 5A). At concentrations greater than a few μM, oscillatory activity was replaced by a slowly declining $[Ca^{2+}]_i$ response. Sensitivity to UTP was also tested to construct the dose–response curve shown in Fig. 5B. The EC_{50} for [UTP] was still submicromolar (72 nM), despite being over two-fold higher than that for [ATP] (23 nM, dashed line, Fig. 5B; see Ref. [33]). We analysed both the amplitude and frequency of the oscillatory activity as a function of concentration. The amplitude of the agonist-induced Ca^{2+} oscillations varied significantly as a function of concentration. The simplest description of the effect of changing concentration on oscillation amplitude is that of an approximate bell shaped function, peaking at ≅50 nM for ATP and ≅250 nM for UTP. Ca^{2+} oscillation frequencies did not appear to alter so consistently and were observed in the range from 0.047 to 0.087 Hz (from 2.84 to 5.22 min^{-1}) for ATP and from 0.034 to 0.07 Hz (from 2.04 to 4.20 min^{-1}) for UTP (Fig. 5E and F). Within these ranges, frequencies did not vary monotonically, albeit the frequencies at which oscillation amplitudes were maximal were similar: 0.06 Hz (3.6 min^{-1}) for ATP and 0.05 Hz (3.0 min^{-1}) for UTP.

ATP, applied at a concentration of 50 nM, reliably elicited Ca^{2+} responses with prominent oscillatory character (Figs. 5A and 6A), whereas ATPγS, 2-MeSATP and UDP failed to evoke measurable fura-2 signals at this concentration (Fig. 6). The responses evoked by ATP, applied at 2 μM concentration, resembled slowly decaying transients. At this higher concentration, ATPγS and 2-MeSATP evoked oscillatory responses whose peak amplitude was only a fraction (70–75%) of the peak ATP response, whereas UDP was ineffective. However, increasing the concentration of UDP to 20 μM resulted in responses of comparable size to that of 2 μM ATP (Fig. 6B).

4. Discussion

ATP levels in scala media increase during brief periods of acoustic overstimulation [25], reaching concentrations above the activation threshold (∼10 nM) for P2YRs in this tissue

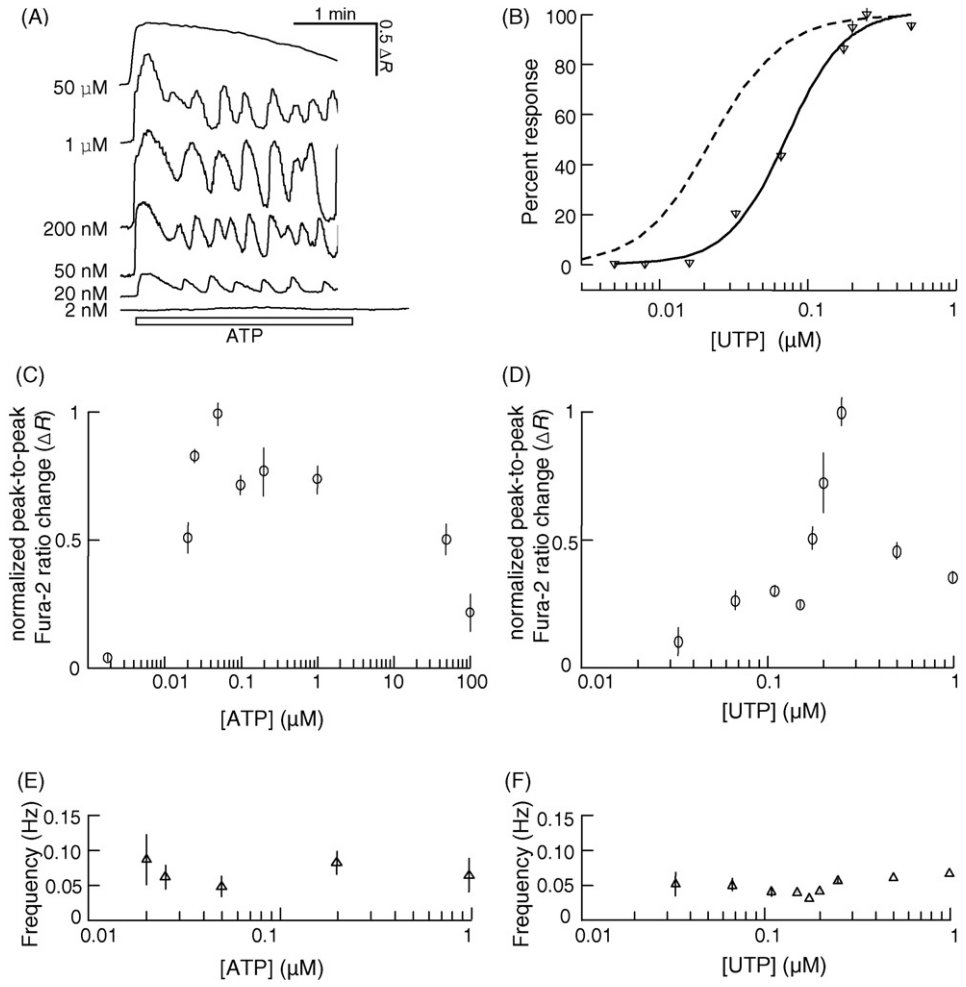

Fig. 5. UTP and ATP affect cochlear supporting cells in a similar way. (A) Representative fura-2 fluorescence ratio changes from individual cells in response to different ATP concentrations, applied for the duration of the recording (empty bar). Each trace was obtained by spatially averaging pixel signals over the whole cell body. (B) Percent dose–response curve for extracellular UTP-induced Ca^{2+} responses; data points (mean ± S.E.M.) are fura-2 signals weighted by the fraction of responding cells in the field of view and averaged over $n > 40$ cells from (at least) three different cultures. Solid line: fit with function $f = 100 \times [UTP]^n/([UTP]^n + k^n)$, where $n = 2.18$ (Hill coefficient) and $k = 0.072$ μM (EC_{50}). Dashed line: ATP dose–response curve from Ref. [33]. (C) Peak-to-peak oscillation amplitudes vs. ATP concentration. (D) Same as (C) for UTP. (E) Oscillation frequency vs. concentration for ATP and UTP (F).

[33]. Signal transduction by P2YRs occurs via the classical pathways triggered by most seven-transmembrane-spanning receptors: (i) agonist-bound receptors determine the rate of G protein activation; (ii) heteromeric G proteins transmit the signal to PLC-β by transiting a controlled cycle of GTP binding and hydrolysis; (iii) G protein-initiated signaling is turned off by hydrolysis of the GTP bound to the Gα subunit.

Our results indicate that Hensen's, Böttcher's and Claudius' cells in the mammalian cochlea are stimulated by ATP in the nanomolar range and once stimulated display a complex pattern of intracellular oscillations and intercellular Ca^{2+} waves. A widely held hypothesis is that, in Ca^{2+} oscillations, information is encoded mainly by their frequency [65–69]. However, a possible role of the amplitude of the Ca^{2+} oscillation in signal transduction has been discussed [70–72]. It has also been argued that amplitude modulation and frequency modulation regulate distinct targets differentially [73].

Feedback processes and cooperativity are the two main sources of non-linearities that promote the occurrence of sustained oscillations in biological systems [52]. Interestingly, certain models for cyclical increases in Ca^{2+} involving calcium-induced calcium release (CICR) have discounted the contribution of Ca^{2+}-dependent PLC activation [74,75]. In a simple two-variable model based on CICR sustained Ca^{2+} oscillations occurred optimally between two critical values of agonist concentration [76], as indeed found in the organ of Corti between 20 nM and 1 μM ATP (see Fig. 5A). However, the model also predicts that the frequency of Ca^{2+} oscillations rises with the degree of stimulation. Here, Ca^{2+} oscillation amplitudes and frequencies displayed complex bi or

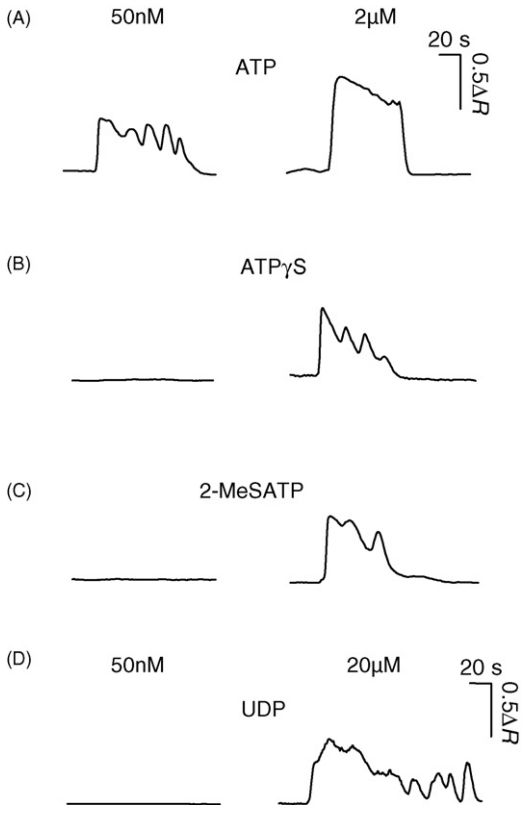

Fig. 6. Sensitivity of supporting cells to agonists of P2 receptors. Fura-2 fluorescence ratio changes, ΔR, from individual supporting cells in response to ATP (A), ATPγS (B), 2-MeSATP (C), and UDP (D) at shown concentrations. Each trace is representative of $n > 3$ experiments.

even triphasic dependence on stimulus concentration: amplitudes peaked at ∼50 nM (ATP, Fig. 5C) and ∼250 nM (UTP, Fig. 5D) whereas the frequency of oscillations appeared to be relatively independent of agonist concentration at ∼0.05 Hz (3 min^{-1}, period 20 s). Furthermore, due to the lack of effect of ryanodine described herein our data are incompatible with a scheme involving ryanodine receptors in the CICR process.

The complex scenario illustrated in Fig. 5 suggests that Ca^{2+} oscillation amplitude and frequency are influenced by a cohort of regulatory and feedback mechanisms, which may include activation and inhibition of the IP_3 receptor at different Ca^{2+} levels [52], as well as regulation of both PLC and G proteins by Ca^{2+} itself [77]. It is critically important for sustained Ca^{2+} oscillations that: (a) PLC-β is a GTPase-activating protein for G_q capable of accelerating steady state GTP-ase activity up to 60-fold [78]; (b) activated α subunits of G_q proteins interact with PLC isozymes at their C2 domains, a class of Ca^{2+} binding modules found in a number of signal transduction proteins [79]. Thus P2YRs and PLC-β may coordinately regulate the amplitude of the Ca^{2+} signal and the rate of signal termination [77].

The expression of specific isoforms of P2YRs may also play a significant role in shaping the spatio-temporal aspects of Ca^{2+} signaling in the network of cells participating in a Ca^{2+} wave [80]. Based on the results described here we suggest the following potency at the native receptors expressed by Hensen's, Böttcher's and Claudius' cells in the cochlear outer sulcus: ATP ≥ UTP ≫ ATPγS = 2-MeSATP ≥ UDP. From this we can conclude that $P2Y_1$, $P2Y_6$ and $P2Y_{11–14}$ are either absent or play a negligible role. Taken together, our results suggest that $P2Y_2$ and $P2Y_4$ receptors, expressed on the endolymphatic side of cochlear supporting cells in the outer sulcus, mediate the observed Ca^{2+} responses. Since P2YRs may form homo- and hetero-multimeric assemblies under some conditions [6], it is tempting to speculate that the unusually high sensitivity to ATP and UTP in this tissue is the result of a peculiar multimerization.

The significance of Ca^{2+} waves and oscillations is intimately connected to the role played by Ca^{2+} in the control of key cellular processes [81]. The extraordinary sensitivity to ATP exhibited by cochlear supporting and epithelial cells in these neonatal cultures suggests that the spreading of intercellular Ca^{2+} waves through the syncytium formed by these cells is an essential component for the perception of sound and is potentially implicated in sound-induced gene expression [33]. However it remains to be determined whether the expression of P2Y receptors is changed during maturation of the cochlea. A detailed study of the expression of P2 receptor expression during cochlea development has not been performed. There is evidence for both change and maintenance of expression of P2X receptors during development [4,80] but data on the expression of P2Y receptors in the organ of Corti is less extensive. P2Y receptors are expressed by supporting cells in the neonatal rat [33] and in the mature guinea pig organ of Corti [8–11,79]. Immunocytochemistry has revealed expression of $P2Y_2$ receptors in the neonatal rat organ [33] and $P2Y_4$ receptors have been found in the adult guinea pig organ [82]. Thus we hypothesize that the mature rat support cells maintain expression of this highly sensitive P2Y based receptor mechanism but a thorough characterization during development is required to confirm this.

A role for these intercellular calcium waves in both cochlear homeostasis, via control of potassium recycling by outer sulcus cells, and in potential repair mechanisms that could be required post-noise trauma is suggested. On-going studies will reveal more of the implications of this mode of cell–cell communication in the inner ear in the near future.

Acknowledgements

Control experiments in Fig. 3A and C were performed by Fabio Anselmi. This work has been supported by grants to FM from Telethon Italy (GGP05131) and the European commission FP6 Integrated Project EuroHear (LSHG-CT-20054-512063) under the Sixth Research Frame Program of The European Union and by a Royal Society University Research Fellowship to JEG. We thank Tullio Pozzan, Bruce Tempel and Luigia Santella for helpful comments and constructive criciticism.

References

[1] P.R. Thorne, G.D. Housley, Purinergic signalling in sensory systems, Semin. Neurosci. 8 (1996) 233–246.

[2] V. Ralevic, G. Burnstock, Receptors for purines and pyrimidines, Pharmacol. Rev. 50 (1998) 413–492.

[3] A. Szucs, H. Szappanos, A. Toth, Z. Farkas, G. Panyi, L. Csernoch, I. Sziklai, Differential expression of purinergic receptor subtypes in the outer hair cells of the guinea pig, Hear. Res. 196 (2004) 2–7.

[4] G.D. Housley, R. Kanjhan, N.P. Raybould, D. Greenwood, S.G. Salih, L. Jarlebark, L.D. Burton, V.C. Setz, M.B. Cannell, C. Soeller, D.L. Christie, S. Usami, A. Matsubara, H. Yoshie, A.F. Ryan, P.R. Thorne, Expression of the P2X(2) receptor subunit of the ATP-gated ion channel in the cochlea: implications for sound transduction and auditory neurotransmission, J. Neurosci. 19 (1999) 8377–8388.

[5] G. Burnstock, Introduction: P2 receptors, Curr. Top. Med. Chem. 4 (2004) 793–803.

[6] G. Burnstock, Purinergic signalling, Br. J. Pharmacol. 147 (Suppl. 1) (2006) S172–S181.

[7] F. Mammano, G.I. Frolenkov, L. Lagostena, I.A. Belyantseva, M. Kurc, V. Dodane, A. Colavita, B. Kachar, ATP-Induced Ca^{2+} release in cochlear outer hair cells: localization of an inositol triphosphate-gated Ca^{2+} store to the base of the sensory hair bundle, J. Neurosci. 19 (1999) 6918–6929.

[8] D. Dulon, R. Moataz, P. Mollard, Characterization of Ca^{2+} signals generated by extracellular nucleotides in supporting cells of the organ of Corti, Cell Calcium 14 (1993) 245–254.

[9] C. Chen, R.P. Bobbin, P2X receptors in cochlear Deiters' cells, Br. J. Pharmacol. 124 (1998) 337–344.

[10] L. Lagostena, F. Mammano, Intracellular calcium dynamics and membrane conductance changes evoked by Deiters' cell purinoceptor activation in the organ of Corti, Cell Calcium 29 (2001) 191–198.

[11] L. Lagostena, J.F. Ashmore, B. Kachar, F. Mammano, Purinergic control of intercellular communication between Hensen's cells of the guinea pig cochlea, J. Physiol. 531 (2001) 693–706.

[12] J.W. Chung, J. Schacht, ATP and nitric oxide modulate intracellular calcium in isolated pillar cells of the guinea pig cochlea, J. Assoc. Res. Otolaryngol. 2 (2001) 399–407.

[13] M. Cohen-Salmon, T. Ott, V. Michel, J.P. Hardelin, I. Perfettini, M. Eybalin, T. Wu, D.C. Marcus, P. Wangemann, K. Willecke, C. Petit, Targeted ablation of connexin26 in the inner ear epithelial gap junction network causes hearing impairment and cell death, Curr. Biol. 12 (2002) 1106–1111.

[14] D.J. Lim, Functional structure of the organ of Corti: a review, Hear Res. 22 (1986) 117–146.

[15] R. Glueckert, K. Pfaller, A. Kinnefors, H. Rask-Andersen, A. Schrott-Fischer, Ultrastructure of the normal human organ of Corti. New anatomical findings in surgical specimens, Acta Otolaryngol. 125 (2005) 534–539.

[16] F. Mammano, S.J. Goodfellow, E. Fountain, Electrophysiological properties of Hensen's cells investigated in situ, Neuroreport 7 (1996) 537–542.

[17] L. Lagostena, A. Cicuttin, J. Inda, B. Kachar, F. Mammano, Frequency dependence of electrical coupling in Deiters' cells of the guinea pig cochlea, Cell Commun. Adhes. 8 (2001) 393–399.

[18] M. Anniko, R. Wroblewski, Ionic environment of cochlear hair cells, Hear Res. 22 (1986) 279–293.

[19] S.Y. Lin, D.P. Corey, TRP channels in mechanosensation, Curr. Opin. Neurobiol. 15 (2005) 350–357.

[20] D.P. Corey, A.J. Hudspeth, Ionic basis of the receptor potential in a vertebrate hair cell, Nature 281 (1979) 675–677.

[21] T.J. Jentsch, Neuronal KCNQ potassium channels: physiology and role in disease, Nat. Rev. Neurosci. 1 (2000) 21–30.

[22] T. Boettger, C.A. Hubner, H. Maier, M.B. Rust, F.X. Beck, T.J. Jentsch, Deafness and renal tubular acidosis in mice lacking the K–Cl co-transporter Kcc4, Nature 416 (2002) 874–878.

[23] G.D. Housley, D. Greenwood, J.F. Ashmore, Localization of cholinergic and purinergic receptors on outer hair cells isolated from the guinea pig cochlea, Proc. R Soc. Lond. B Biol. Sci. 249 (1992) 265–273.

[24] G.D. Housley, D.J. Jagger, D. Greenwood, N.P. Raybould, S.G. Salih, L.E. Jarlebark, S.M. Vlajkovic, R. Kanjhan, P. Nikolic, D.J. Munoz, P.R. Thorne, Purinergic regulation of sound transduction and auditory neurotransmission, Audiol. Neurootol. 7 (2002) 55–61.

[25] D.J. Munoz, I.S. Kendrick, M. Rassam, P.R. Thorne, Vesicular storage of adenosine triphosphate in the guinea pig cochlear lateral wall and concentrations of ATP in the endolymph during sound exposure and hypoxia, Acta Otolaryngol. 121 (2001) 10–15.

[26] P.N. White, P.R. Thorne, G.D. Housley, B. Mockett, T.E. Billett, G. Burnstock, Quinacrine staining of marginal cells in the stria vascularis of the guinea pig cochlea: a possible source of extracellular ATP? Hear. Res. 90 (1995) 97–105.

[27] L.E. Jarlebark, G.D. Housley, N.P. Raybould, S. Vlajkovic, P.R. Thorne, ATP-gated ion channels assembled from P2X2 receptor subunits in the mouse cochlea, Neuroreport 13 (2002) 1979–1984.

[28] Y. Osipchuk, M. Cahalan, Cell-to-cell spread of calcium signals mediated by ATP receptors in mast cells, Nature 359 (1992) 241–244.

[29] F. Di Virgilio, P. Chiozzi, D. Ferrari, S. Falzoni, J.M. Sanz, A. Morelli, M. Torboli, G. Bolognesi, O.R. Baricordi, Nucleotide receptors: an emerging family of regulatory molecules in blood cells, Blood 97 (2001) 587–600.

[30] H.M. Sobkowicz, J.M. Loftus, S.M. Slapnick, Tissue culture of the organ of Corti, Acta Otolaryngol. 502 (Suppl.) (1993) 3–36.

[31] H.M. Sobkowicz, B. Bereman, J.E. Rose, Organotypic development of the organ of Corti in culture, J. Neurocytol. 4 (1975) 543–572.

[32] G.P. Richardson, I.J. Russell, Cochlear cultures as a model system for studying aminoglycoside induced ototoxicity, Hear. Res. 53 (1991) 293–311.

[33] J.E. Gale, V. Piazza, C.D. Ciubotaru, F. Mammano, A mechanism for sensing noise damage in the inner ear, Curr. Biol. 14 (2004) 526–529.

[34] A.H. Cornell-Bell, S.M. Finkbeiner, M.S. Cooper, S.J. Smith, Glutamate induces calcium waves in cultured astrocytes: long-range glial signaling, Science 247 (1990) 470–473.

[35] M.J. Sanderson, A.C. Charles, E.R. Dirksen, Mechanical stimulation and intercellular communication increases intracellular Ca^{2+} in epithelial cells, Cell Regul. 1 (1990) 585–596.

[36] M. Tachibana, H. Morioka, Well developed gap junctions between Deiter's cells of the organ of Corti, J. Electr. Microsc. (Tokyo) 25 (1976) 95–97.

[37] T. Kikuchi, R.S. Kimura, D.L. Paul, J.C. Adams, Gap junctions in the rat cochlea: immunohistochemical and ultrastructural analysis, Anat. Embryol. (Berlin) 191 (1995) 101–118.

[38] T. Kikuchi, R.S. Kimura, D.L. Paul, T. Takasaka, J.C. Adams, Gap junction systems in the mammalian cochlea, Brain Res. Brain Res. Rev. 32 (2000) 163–166.

[39] N.L. Allbritton, T. Meyer, Localized calcium spikes and propagating calcium waves, Cell Calcium 14 (1993) 691–697.

[40] J.C. Saez, J.A. Connor, D.C. Spray, M.V. Bennett, Hepatocyte gap junctions are permeable to the second messenger, inositol 1,4,5-trisphosphate, and to calcium ions, Proc. Natl. Acad. Sci. U.S.A. 86 (1989) 2708–2712.

[41] N.L. Allbritton, T. Meyer, L. Stryer, Range of messenger action of calcium ion and inositol 1,4,5-trisphosphate, Science 258 (1992) 1812–1815.

[42] J. Sneyd, B.T. Wetton, A.C. Charles, M.J. Sanderson, Intercellular calcium waves mediated by diffusion of inositol trisphosphate: a two-dimensional model, Am. J. Physiol. 268 (1995) C1537–C1545.

[43] T. Tordjmann, B. Berthon, M. Claret, L. Combettes, Coordinated intercellular calcium waves induced by noradrenaline in rat hepatocytes: dual control by gap junction permeability and agonist, EMBO J. 16 (1997) 5398–5407.

[44] A.C. Charles, C.C. Naus, D. Zhu, G.M. Kidder, E.R. Dirksen, M.J. Sanderson, Intercellular calcium signaling via gap junctions in glioma cells, J. Cell Biol. 118 (1992) 195–201.

[45] A. Verkhratsky, H. Kettenmann, Calcium signalling in glial cells, Trends Neurosci. 19 (1996) 346–352.
[46] C. Giaume, L. Venance, Intercellular calcium signaling and gap junctional communication in astrocytes, Glia 24 (1998) 50–64.
[47] L. Venance, N. Stella, J. Glowinski, C. Giaume, Mechanism involved in initiation and propagation of receptor-induced intercellular calcium signaling in cultured rat astrocytes, J. Neurosci. 17 (1997) 1981–1992.
[48] E.A. Newman, K.R. Zahs, Calcium waves in retinal glial cells, Science 275 (1997) 844–847.
[49] E.A. Newman, Propagation of intercellular calcium waves in retinal astrocytes and Muller cells, J. Neurosci. 21 (2001) 2215–2223.
[50] S. Bastianello, C.D. Ciubotaru, M. Beltramello, F. Mammano, Dissecting key components of the Ca^{2+} homeostasis game by multi-functional fluorescence imaging, Proc. SPIE 5324 (2004) 265–274.
[51] S.O. Suadicani, C.F. Brosnan, E. Scemes, P2X7 receptors mediate ATP release and amplification of astrocytic intercellular Ca^{2+} signaling, J. Neurosci. 26 (2006) 1378–1385.
[52] A. Goldbeter, Computational approaches to cellular rhythms, Nature 420 (2002) 238–245.
[53] M.J. Berridge, Inositol trisphosphate and calcium signalling, Nature 361 (1993) 315–325.
[54] J.M. Reifel Saltzberg, K.A. Garvey, S.A. Keirstead, Pharmacological characterization of P2Y receptor subtypes on isolated tiger salamander Muller cells, Glia 42 (2003) 149–159.
[55] K. Chang, K. Hanaoka, M. Kumada, Y. Takuwa, Molecular cloning and functional analysis of a novel P2 nucleotide receptor, J. Biol. Chem. 270 (1995) 26152–26158.
[56] S.J. Charlton, C.A. Brown, G.A. Weisman, J.T. Turner, L. Erb, M.R. Boarder, Cloned and transfected P2Y4 receptors: characterization of a suramin and PPADS-insensitive response to UTP, Br. J. Pharmacol. 119 (1996) 1301–1303.
[57] D. Communi, S. Motte, J.M. Boeynaems, S. Pirotton, Pharmacological characterization of the human P2Y4 receptor, Eur. J. Pharmacol. 317 (1996) 383–389.
[58] D. Communi, M. Parmentier, J.M. Boeynaems, Cloning, functional expression and tissue distribution of the human P2Y6 receptor, Biochem. Biophys. Res. Commun. 222 (1996) 303–308.
[59] K.D. Lustig, A.K. Shiau, A.J. Brake, D. Julius, Expression cloning of an ATP receptor from mouse neuroblastoma cells, Proc. Natl. Acad. Sci. U.S.A. 90 (1993) 5113–5117.
[60] Y.D. Bogdanov, S.S. Wildman, M.P. Clements, B.F. King, G. Burnstock, Molecular cloning and characterization of rat P2Y4 nucleotide receptor, Br. J. Pharmacol. 124 (1998) 428–430.
[61] K. Ayyanathan, T.E. Webbs, A.K. Sandhu, R.S. Athwal, E.A. Barnard, S.P. Kunapuli, Cloning and chromosomal localization of the human P2Y1 purinoceptor, Biochem. Biophys. Res. Commun. 218 (1996) 783–788.
[62] D.J. Henderson, D.G. Elliot, G.M. Smith, T.E. Webb, I.A. Dainty, Cloning and characterisation of a bovine P2Y receptor, Biochem. Biophys. Res. Commun. 212 (1995) 648–656.
[63] D. Communi, C. Govaerts, M. Parmentier, J.M. Boeynaems, Cloning of a human purinergic P2Y receptor coupled to phospholipase C and adenylyl cyclase, J. Biol. Chem. 272 (1997) 31969–31973.
[64] M.P. Abbracchio, G. Burnstock, Purinoceptors: are there families of P2X and P2Y purinoceptors? Pharmacol. Ther. 64 (1994) 445–475.
[65] T. Meyer, L. Stryer, Molecular model for receptor-stimulated calcium spiking, Proc. Natl. Acad. Sci. U.S.A. 85 (1988) 5051–5055.
[66] G. Dupont, A. Goldbeter, CaM kinase II as frequency decoder of Ca^{2+} oscillations, Bioessays 20 (1998) 607–610.
[67] M. Marhl, S. Schuster, M. Brumen, Mitochondria as an important factor in the maintenance of constant amplitudes of cytosolic calcium oscillations, Biophys. Chem. 2 (1998) 125–132.
[68] U. Kummer, L.F. Olsen, C.J. Dixon, A.K. Green, E. Bornberg-Bauer, G. Baier, Switching from simple to complex oscillations in calcium signalling, Biophys. J. 79 (2000) 1188–1195.
[69] Y. Tang, H.G. Othmer, Frequency encoding in excitable systems with applications to calcium oscillations, Proc. Natl. Acad. Sci. U.S.A. 92 (1995) 7869–7873.
[70] C. Schofl, G. Brabant, R.D. Hesch, A. von zur Muhlen, P.H. Cobbold, K.S. Cuthbertson, Temporal patterns of alpha 1-receptor stimulation regulate amplitude and frequency of calcium transients, Am. J. Physiol. 265 (1993) C1030–C1036.
[71] R.E. Dolmetsch, R.S. Lewis, C.C. Goodnow, J.I. Healy, Differential activation of transcription factors induced by Ca^{2+} response amplitude and duration, Nature 386 (1997) 855–858.
[72] K. Prank, F. Gabbiani, G. Brabant, Coding efficiency and information rates in transmembrane signaling, Biosystems 55 (2000) 15–22.
[73] M.J. Berridge, The AM and FM of calcium signalling, Nature 386 (1997) 759–760.
[74] A. Atri, J. Amundson, D. Clapham, J. Sneyd, A single-pool model for intracellular calcium oscillations and waves in the *Xenopus laevis* oocyte, Biophys. J. 65 (1993) 1727–1739.
[75] G. Dupont, M.J. Berridge, A. Goldbeter, Signal-induced Ca^{2+} oscillations: properties of a model based on Ca^{2+}-induced Ca^{2+} release, Cell Calcium 12 (1991) 73–85.
[76] A. Goldbeter, G. Dupont, M.J. Berridge, Minimal model for signal-induced Ca^{2+} oscillations and for their frequency encoding through protein phosphorylation, Proc. Natl. Acad. Sci. U.S.A. 87 (1990) 1461–1465.
[77] S.G. Rhee, Regulation of phosphoinositide-specific phospholipase C, Annu. Rev. Biochem. 70 (2001) 281–312.
[78] G.H. Biddlecome, G. Berstein, E.M. Ross, Regulation of phospholipase C-beta1 by Gq and m1 muscarinic cholinergic receptor. Steady-state balance of receptor-mediated activation and GTPase-activating protein-promoted deactivation, J. Biol. Chem. 271 (1996) 7999–8007.
[79] T. Wang, S. Pentyala, J.T. Elliott, L. Dowal, E. Gupta, M.J. Rebecchi, S. Scarlata, Selective interaction of the C2 domains of phospholipase C-beta1 and -beta2 with activated Galphaq subunits: an alternative function for C2-signaling modules, Proc. Natl. Acad. Sci. U.S.A. 96 (1999) 7843–7846.
[80] C.J. Gallagher, M.W. Salter, Differential properties of astrocyte calcium waves mediated by P2Y1 and P2Y2 receptors, J. Neurosci. 23 (2003) 6728–6739.
[81] M.J. Berridge, Elementary and global aspects of calcium signalling, J. Physiol. 499 (Pt 2) (1997) 291–306.
[82] M.S. Parker, N.N. Onyenekwu, R.P. Bobbin, Localization of the P2Y4 receptor in the guinea pig organ of Corti, J. Am. Acad. Audiol. 14 (2003) 286–295.